Cellular mechanism of insulin resistance in nonalcoholic fatty liver disease

Naoki Kumashiro[a,b], Derek M. Erion[a,b,c], Dongyan Zhang[a], Mario Kahn[b], Sara A. Beddow[b], Xin Chu[d], Christopher D. Still[d], Glenn S. Gerhard[d], Xianlin Han[e], James Dziura[b], Kitt Falk Petersen[b], Varman T. Samuel[b,f,1], and Gerald I. Shulman[a,b,c,1]

[a]Howard Hughes Medical Institute and Departments of [b]Internal Medicine and [c]Cellular and Molecular Physiology, Yale University School of Medicine, New Haven, CT 06510; [d]Weis Center for Research, Geisinger Clinic, Danville, PA 17822; [e]Diabetes and Obesity Research Center, Sanford-Burnham Medical Research Institute, Orlando, FL 32827; and [f]Veterans Affairs Medical Center, West Haven, CT 06516

Contributed by Gerald I. Shulman, August 24, 2011 (sent for review July 22, 2011)

Insulin resistance is associated with nonalcoholic fatty liver disease (NAFLD) and is a major factor in the pathogenesis of type 2 diabetes. The development of hepatic insulin resistance has been ascribed to multiple causes, including inflammation, endoplasmic reticulum (ER) stress, and accumulation of hepatocellular lipids in animal models of NAFLD. However, it is unknown whether these same cellular mechanisms link insulin resistance to hepatic steatosis in humans. To examine the cellular mechanisms that link hepatic steatosis to insulin resistance, we comprehensively assessed each of these pathways by using flash-frozen liver biopsies obtained from 37 obese, nondiabetic individuals and correlating key hepatic and plasma markers of inflammation, ER stress, and lipids with the homeostatic model assessment of insulin resistance index. We found that hepatic diacylglycerol (DAG) content in cytoplasmic lipid droplets was the best predictor of insulin resistance ($R = 0.80$, $P < 0.001$), and it was responsible for 64% of the variability in insulin sensitivity. Hepatic DAG content was also strongly correlated with activation of hepatic PKCε ($R = 0.67$, $P < 0.001$), which impairs insulin signaling. In contrast, there was no significant association between insulin resistance and other putative lipid metabolites or plasma or hepatic markers of inflammation. ER stress markers were only partly correlated with insulin resistance. In conclusion, these data show that hepatic DAG content in lipid droplets is the best predictor of insulin resistance in humans, and they support the hypothesis that NAFLD-associated hepatic insulin resistance is caused by an increase in hepatic DAG content, which results in activation of PKCε.

Hepatic insulin resistance is associated with nonalcoholic fatty liver disease (NAFLD) and is a major factor in the pathogenesis of type 2 diabetes (T2D) and the metabolic syndrome (1–3). Although there is general consensus that insulin resistance is caused by defects in intracellular insulin signaling, multiple causes have been proposed to explain how these insulin signaling defects arise in NAFLD. Inflammation, activation of endoplasmic reticulum (ER) stress pathways, and accumulation of hepatocellular lipids have all been suggested to cause insulin resistance in animal models of NAFLD (Fig. S1) (4–7). First, intracellular diacylglycerols (DAGs) can inhibit insulin signaling by activation of novel PKC isoforms (6, 8, 9), which in turn, block insulin receptor kinase phosphorylation of insulin receptor substrates 1 and 2. Intracellular ceramides are thought to prevent Akt2 activation (10–12) (Fig. S1). Second, adipocytokines (e.g., TNF-α, IL-1β, and IL-6) interfere with insulin signaling through activation of the JNK or inhibitor of IκB kinase-β pathways (13–15). Finally, the unfolded protein response, or ER stress pathways are also implicated in the pathogenesis of insulin resistance. This response is initiated with the disassociation of immunoglobulin heavy-chain binding protein (BiP) from key mediators of a coordinated ER stress pathway, dsRNA-activated kinase-like ER kinase (PERK), activating transcription factor (ATF) 6, and inositol requiring ER to nucleus signal kinase (IRE) 1α. The latter has been reported to impair insulin signaling by activation of JNK (14, 16). Although animal studies have supported each of these hypotheses, few studies have examined these potential mechanisms in a comprehensive fashion in humans. Therefore, whether these same mechanisms translate to humans with NAFLD is unknown.

To determine whether any of these putative mechanisms for insulin resistance translate to humans, we assessed these potential pathways in liver tissue obtained from nondiabetic obese individuals undergoing bariatric surgery. Under these conditions, fresh liver biopsies could safely be obtained in sufficient quantities to determine the potential hepatic cellular and molecular changes that relate to insulin resistance in humans.

Results

Participant Characteristics. We studied 37 obese, nondiabetic (hemoglobin $A_{1C} < 6.5\%$) subjects (Table 1). As an aggregate, these subjects were insulin-resistant, which was assessed by the homeostatic model assessment of insulin resistance index (HOMA-IR; 4.6 ± 2.2 mg/dL × μU/mL; normal < 2.0 mg/dL × μU/mL) (17). However, the individuals within this cohort had a large range of values (1.4–9.3 mg/dL × μU/mL), showing that some remain insulin-sensitive despite being morbidly obese. The analyses that we performed sought to understand what factors best predicted the variation of the insulin resistance in these individuals.

Hepatic DAG Content and Insulin Resistance. As in subjects with lesser degrees of obesity, there was a positive but relatively weak association ($R = 0.39$) between body mass index (BMI) and HOMA-IR (Fig. 1*A*) (18). Using flash-frozen liver specimens, we comprehensively assessed whether changes in lipid species, activation of the unfolded protein response, or systemic or tissue inflammation could better account for insulin resistance in this cohort. The intrahepatic concentrations of long-chain fatty acyl-CoAs (LCCoAs) or ceramides did not relate to HOMA-IR (Fig. 1 *E* and *F*). In contrast, hepatic DAG content was found to be strongly and positively correlated with HOMA-IR ($R = 0.73$, $P < 0.001$) (Fig. 1*B*). DAGs are present as constituent lipids within either the plasma membrane or cytosolic lipid droplets (19). Liver samples were separated into membrane and cytosolic lipid droplet compartments, and DAG was quantified again. Surprisingly, the DAG content in lipid droplets correlated with HOMA-IR strongly ($R = 0.80$, $P < 0.001$) (Fig. 1*C*), and the correlation was stronger than either membrane DAG or total DAG content (Fig. 1 *B* and *D*). The relationship between DAG content in lipid

Author contributions: N.K., K.F.P., V.T.S., and G.I.S. designed research; N.K., D.M.E., D.Z., M.K., S.A.B., X.C., C.D.S., G.S.G., and X.H. performed research; X.C., C.D.S., G.S.G., X.H., and J.D. contributed new reagents/analytic tools; N.K., D.M.E., D.Z., M.K., S.A.B., C.D.S., G.S.G., X.H., J.D., K.F.P., V.T.S., and G.I.S. analyzed data; and N.K., G.S.G., K.F.P., V.T.S., and G.I.S. wrote the paper.

The authors declare no conflict of interest.

Freely available online through the PNAS open access option.

[1]To whom correspondence may be addressed. E-mail: varman.samuel@yale.edu or gerald.shulman@yale.edu.

This article contains supporting information online at www.pnas.org/lookup/suppl/doi:10.1073/pnas.1113359108/-/DCSupplemental.

Table 1. Characteristics of participants

Characteristic	Number
Total number	37
Female (%)	28 (75.7)
Age (y)	42.0 (13.2)
BMI (kg/m^2)	48.4 (8.8)
Fasting plasma glucose (mg/dL)	97.1 (14.0)
Fasting plasma insulin (μU/mL)	21.1 (7.8)
HbA_{1C} (%)	5.6 (0.4)
HOMA-IR (mg/dL × μU/mL)	4.6 (2.2)
Alanine aminotransferase (IU/L)	27.8 (12.7)
Aspartate aminotransferase (IU/L)	24.3 (6.7)
LDL cholesterol (mg/dL)	103 (36.0)
HDL cholesterol (mg/dL)	43.3 (9.0)
Triglyceride (mg/dL)	149 (92.0)

SI conversion factors: To convert HDL and LDL to mmol/L, multiply by 0.0259; to convert triglyceride to mmol/L, multiply by 0.0113. Data are expressed as mean (SD) unless otherwise indicated. HbA_{1C}, hemoglobin A_{1C}; HDL, high-density lipoprotein; HOMA-IR, homeostatic model assessment of insulin resistance index; LDL, low-density lipoprotein.

droplets or total DAG and HOMA-IR was unaffected after adjusting for age, sex, and BMI. Membrane DAG had no significant correlation with HOMA-IR when each sex was analyzed separately. We also analyzed individual DAG species in relation to HOMA-IR. As shown in Table S1, DAGs composed of C18:1–C16:0, C18:1–C18:1, C18:1–C18:2, and C16:0–C18:2 were most abundant and also strongly related with HOMA-IR. Interestingly, the content of DAG composed of C20:4–C20:5 showed a strong negative correlation with HOMA-IR. We also performed a comprehensive lipidomics screen to assess changes in other lipid species using a subset of the most insulin-sensitive and -resistant individuals (Dataset S1). However, none of the measured species exhibited significant differences except for in the concentration of some fatty acids found in triglyceride, which likely mirrors the changes in DAG species (Fig. S2*A*).

DAG in Lipid Droplet and PKCε Activation. DAGs mediate insulin resistance through activation of PKCs, specifically the novel isoforms PKCδ, -ε, and -θ (Fig. S1) (4, 6, 9, 20, 21). A comprehensive analysis of PKC isoforms in human liver has not previously been reported. Thus, we assessed activation of all PKC isoforms in relation to insulin resistance and lipid content using a translocation assay in which the abundance of a PKC isoform in the membrane compartment is compared with the cytosolic compartment as an index of activation (8).

PKCε was one of the major PKC isoforms expressed in human liver along with PKCα, -β, -ζ, -ι, and -δ, whereas PKCη, -θ, and -γ were not detected. PKCε activation was also strongly correlated with hepatic DAG content in lipid droplets (Fig. 2*A*). By comparison, there was no association between activation of PKCα, -β, -δ, or -ι and hepatic DAG content (Table S2). Although PKCε was found to exist primarily in membrane fraction and have relatively very low expression in cytosol, PKCε was also strongly detected in the lipid droplet fraction in cytosol, whereas other isoforms were not (Fig. 2*C*). This suggests that PKCε is bound to DAG in lipid droplet in cytosol, thus activating and translocating to the membrane. Finally, we also observed that activation of PKCζ positively correlated with the DAG content in lipid droplet ($P = 0.02$) (Table S2), but the degree of activation was lower compared with PKCε. Consistent with this difference in activation, we also found a strong correlation between PKCε activation and HOMA-IR ($R = 0.55$, $P < 0.001$) but no correlation between PKCζ activation and HOMA-IR.

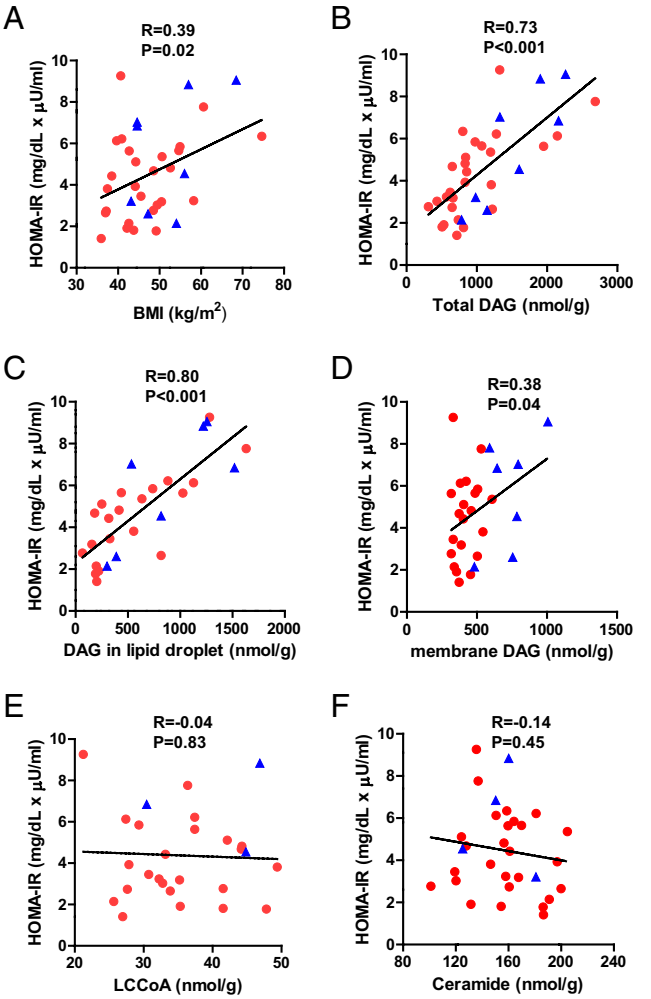

Fig. 1. DAG content in lipid droplets was the strongest predictor of insulin resistance. DAG, diacylglycerol; HOMA-IR, homeostatic model assessment of insulin resistance index; LCCoA, long-chain fatty acyl-CoA. Red dots and blue triangles show females and males, respectively. n = 35, 35, 28, 28, 28, and 32 for *A*, *B*, *C*, *D*, *E*, and *F*, respectively.

Unfolded Protein Response and Insulin Resistance. The ER is the major site in the cell for protein folding and trafficking. The accumulation of unfolded proteins within the ER initiates the unfolded protein response with the disassociation of BiP from three key proteins, PERK, ATF6, and IRE1α (Fig. S1). These proteins subsequently activate downstream unfolded protein response pathways to coordinate adaptive responses that decrease the presence of unfolded proteins and expand the ER. Phosphorylation of the eukaryotic translation initiation factor (eIF2α), a reaction that is catalyzed by PERK, increased with worsening insulin resistance (Fig. 3*A*). eIF2α phosphorylation, in turn, should activate a set of downstream targets, such as ATF4, ATF3, and CCAAT/enhancer binding protein homologous protein (CHOP) mRNA, but with the exception of CHOP protein expression (Fig. 3*B*), there was no relationship between the expression of these other ER stress factors and HOMA-IR (Table S3). The ATF6 pathway is activated through ATF6 cleavage at the Golgi apparatus and positively regulates CHOP expression (Fig. S1). Surprisingly, in contrast to CHOP protein expression, we found that ATF6 cleavage tended to be decreased in relation to HOMA-IR (Table S3). Activation of the IRE1α pathway leads to X-box binding protein-1 (XBP1) splicing and JNK phosphoryla-

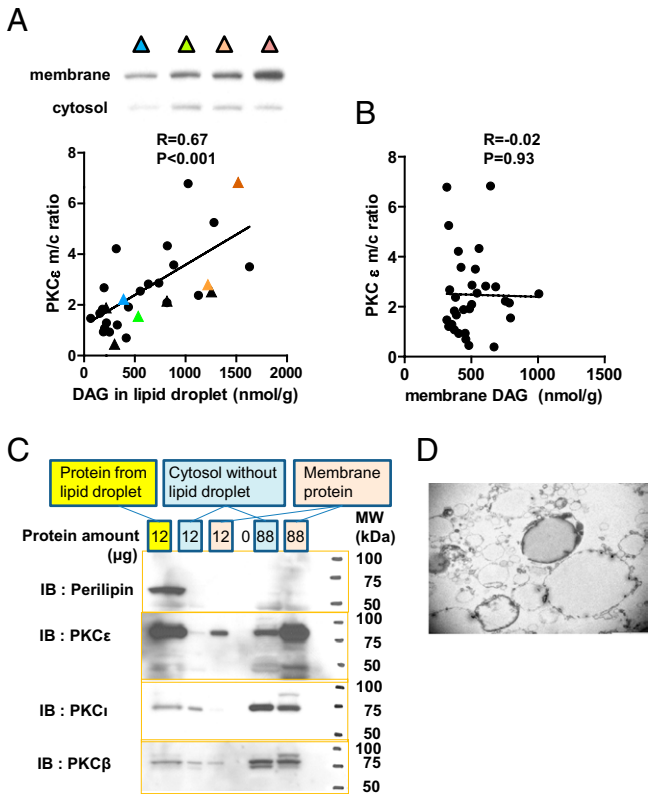

Fig. 2. PKCε activation was strongly correlated with DAG content in lipid droplets. m/c, membrane/cytosol. Representative bands are labeled with colors and shown with corresponding colors on the graph (*A*). Circles and triangles show females and males, respectively (*A*). $n = 30$ for both A and *B*. Lipid droplet fraction was confirmed with Western blotting (*C*) and EM (*D*).

tion and activation. However, we found that neither the expression of spliced XBP1 mRNA nor JNK phosphorylation, which is most often implicated in the pathogenesis of insulin resistance in rodent models (15), had any relation to HOMA-IR (Table S3).

Markers of Inflammation and Insulin Resistance. Numerous studies have implicated inflammation as a major causal factor in promoting insulin resistance through activation of JNK, which is a common node in both ER stress and the inflammatory pathways (15, 22, 23). However, as noted, we did not observe any relationship between JNK activation with insulin resistance in these subjects. We also sought to determine whether other inflammatory pathways might be associated with insulin resistance in this cohort. TNFα, IL-1β, and IL-6 have been suggested to be the key cytokines responsible for causing insulin resistance associated with obesity and NAFLD (7, 13, 15, 22, 23). There were no significant correlations between hepatic expression of C-reactive protein (CRP), cytokine mRNA, plasma high-sensitive C-reactive protein (hsCRP), or plasma cytokine concentrations and HOMA-IR (Table S4). Plasma adiponectin concentrations showed a tendency to be inversely related to HOMA-IR (Fig. S3).

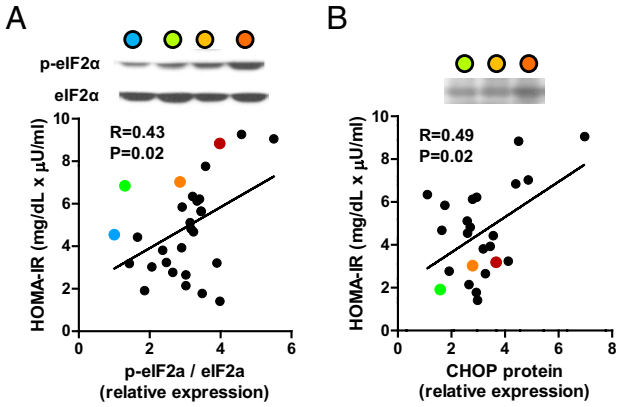

Fig. 3. Correlation between ER stress markers and HOMA-IR. The relative expression level was expressed by setting the lowest expression level as one (*A* and *B*). Representative bands are labeled with colors and shown with corresponding colors on the graph (*A* and *B*). $n = 30$ and 25 for *A* and *B*, respectively.

Discussion

In this study, we assessed the key putative mechanisms responsible for hepatic insulin resistance in humans. Notably, although all of the subjects were morbidly obese, these individuals exhibited a wide range in insulin sensitivity. We comprehensively analyzed plasma and liver tissue from these subjects and examined the three major mechanisms that are currently thought to be responsible for insulin resistance. We found that hepatic DAG content, specifically, DAG content within cytosolic lipid droplets, best accounted for insulin resistance in these individuals ($R = 0.80$, $P < 0.001$) and was responsible for 64% of the variability in insulin sensitivity. Furthermore, the DAG content in lipid droplets was strongly associated with PKCε activation in liver. In contrast, there was no significant association between plasma or hepatic markers of inflammation, putative ER stress markers such as JNK, and hepatic ceramide content and insulin resistance. Taken together, these results support a key role of hepatocellular DAG and PKCε activation in the pathogenesis of insulin resistance in humans and are consistent with studies that have shown a key role for this pathway in causing hepatic insulin resistance in rodent models of NAFLD (6, 9, 24–26).

In executing this study, fresh liver samples were obtained and immediately flash-frozen in liquid nitrogen, thereby avoiding the warm ischemia that may artificially increase intracellular lipid species in liver. In addition to hepatic DAG content, liver triglyceride was also highly correlated with HOMA-IR ($R = 0.67$) (Fig. S2*B*), consistent with previous studies (27). However, triglyceride is considered an inert storage form of lipid, and previous studies in transgenic and gene KO mice have found that intracellular DAGs are the likely mediator of lipid-induced insulin resistance (21, 28). Other lipid species such as ceramides and LCCoAs have also been implicated in causing insulin resistance in liver and skeletal muscle (29–31). However, we did not detect any correlation between hepatic ceramide or LCCoA content and insulin resistance, arguing against a major role for these lipid metabolites in the pathogenesis of hepatic insulin resistance in humans, consistent with previous animal studies (26, 32). Given our findings showing important differences in the subcellular fractions of DAGs in liver and its relationship with insulin resistance, it will be of interest to apply these same subcellular fractionation methods to ceramides.

We hypothesized that DAG content in discrete cellular compartments may contribute differently to the development of insulin resistance. Liver samples were partitioned into membrane and cytosolic compartments; the latter contained the lipid droplets, which was confirmed by immunodetection of perilipin and direct visualization by EM. Surprisingly, the lipid droplet DAG content ($R = 0.80$) and the total DAG content ($R = 0.73$) were very strong predictors of insulin resistance in contrast to a relatively weak relationship between membrane DAG content and insulin resistance ($R = 0.38$). Taken together, these data suggest that DAG in cytosolic lipid droplets may be the active pool of DAGs responsible for causing insulin resistance in humans.

DAGs are thought to impair insulin signaling through activation of novel PKCs (4). We examined the expression and activity

of all known PKC isoforms. As in rodents (9), PKCε was one of the major PKC isoforms present in human liver, and PKCε activation strongly correlated with both lipid droplet DAG content and insulin resistance. Activation of PKCζ was also significantly correlated with hepatic DAG content, but the relationship was weaker than PKCε. Considine et al. (33) previously showed an increase in the membrane abundance of PKCε in patients with T2D; however, in contrast to our study, they did not find an increase in PKCε membrane content in the small number ($n = 5$) of obese, nondiabetic subjects they studied and they did not relate PKCε activity to increases in hepatic DAG content or insulin resistance (33). Thus, this study shows that the DAG–PKCε axis is closely related to insulin resistance in humans.

Activation of the unfolded protein response, or ER stress pathway, has also been implicated to cause hepatic insulin resistance (16, 34). This pathway is initiated with the disassociation of BiP from key mediators of a coordinated ER stress pathway, PERK, IRE, and ATF6. These arms each activate downstream effectors that have been reported to also impair insulin signaling. There was no significant relationship between HOMA-IR and markers of the IRE-1α ER stress pathway (spliced XBP1 mRNA and JNK1, -2, and -3 phosphorylation) (Table S3), which are thought to be the key mediators for insulin resistance in response to ER stress (14, 16). We observed a partial activation of constituent pathways relative to insulin resistance. Specifically, hepatic eIF2α phosphorylation and CHOP protein (both part of the PERK arm) were both positively correlated with HOMA-IR (Fig. 3 *A* and *B*). Growth arrest and DNA damage-inducible protein (GADD) 34 dephosphorylates eIF2α and terminates the signal through this arm. Thus, it is possible that a reduced expression of GADD34 may have contributed to the increase in eIF2α phosphorylation per se. However, there was no significant relationship between either eIF2α phosphorylation or HOMA-IR and GADD34 mRNA expression (Fig. S4 *A* and *B*). Thus, the findings that eIF2α and CHOP relate to insulin resistance in relative isolation from other aspects of the unfolded protein response and the absence of a relationship between JNK1 activation and HOMA-IR argue against a causal role of ER stress in insulin resistance.

Finally, alterations in plasma adipocytokines and tissue inflammation have also been implicated to cause insulin resistance (15, 22, 23, 35). We found no relationship between the plasma concentration or hepatic expression of TNFα, IL-1β, IL-6, or CRP and HOMA-IR, suggesting that these factors do not have a major role in causing insulin resistance in these individuals. Plasma adiponectin concentration showed a tendency to be inversely related to HOMA-IR, specifically in females (Fig. S3).

Although this study strongly supports a key role of hepatocellular DAG and PKCε activation in the pathogenesis of insulin resistance in humans, there are some limitations that need to be discussed. First, this is a correlative study, and we cannot rule out the possibility that hepatic DAG content in lipid droplets and PKCε activation are both secondary to insulin resistance. However, the causal role of DAG-induced PKCε activation in mediating hepatic insulin resistance is supported by multiple animal studies (4, 6, 29, 36). Notably, decreasing PKCε expression in liver, using a specific antisense oligonucleotide, protected rats from hepatic insulin resistance, despite the development of NAFLD (25). Second, HOMA-IR was used as an index of hepatic insulin resistance. Studies by our group (37, 38) and others (39, 40) have established a strong relationship between hepatic triglyceride content and hepatic insulin resistance assessed by the hyperinsulinemic–euglycemic clamp method, and in this study, we found a strong relationship ($R = 0.90$, $P < 0.001$) between hepatic triglyceride and DAG content in our subjects (Fig. S2*A*), which strongly suggests the direct relationship between hepatic DAG content and hepatic insulin resistance. Third, our study was limited to mostly nondiabetic Caucasian individuals with extreme obesity. Thus, future studies will need to extend these findings to leaner individuals of different ethnicities.

In conclusion, these data support the hypothesis that hepatic insulin resistance in humans with NAFLD is caused by an increase in hepatic DAG content in cytosolic lipid droplets, resulting in activation of PKCε. Given that NAFLD is ubiquitously associated with the metabolic syndrome and T2D, these data suggest that therapies designed to reduce hepatic DAG content will be efficacious in treating hepatic insulin resistance associated with NAFLD and T2D.

Materials and Methods

Study Population. All patients who were enrolled in the Bariatric Surgery Program of the Geisinger Center for Nutrition and Weight Management between October 2004 and October 2010 were offered the opportunity to participate in the study (41). Over 90% of patients consented to participate. Patients underwent a preoperative assessment and preparation program of monthly visits, during which time a comprehensive set of clinical and laboratory measures were obtained. Although patients lost an average of ∼9% body weight over the year before surgery, they remained relatively weight stable during the preoperative period between blood sampling and liver biopsy, with an average percent change in body weight of 0.41%. The protocol was approved by the Institutional Review Boards of the Geisinger Clinic and Yale University, and all participants provided written informed consent. For these studies, we primarily studied patients without a history of type 2 diabetes.

Liver Biopsies. During the bariatric surgery, a wedge biopsy (250–300 mg) was obtained from the right lobe of the liver (10 cm to the left of the falciform ligament) and flash-frozen in liquid nitrogen for subsequent analysis. The remainder was divided for routine histology. NAFLD was diagnosed with standard histological criteria (42). Flash-frozen liver samples were then later divided for use to measure key lipid metabolites and gene and protein expression. Because of the small and varying size of the liver sample, not every analysis could be performed on every subject.

Hepatic Lipid Metabolites Assay. Hepatic triglyceride content was determined by using a triglyceride assay kit (Genzyme) and a method adapted from the work by Storlien et al. (43). The extraction, purification, and assessment of medium-, long-, and very long-chain fatty acyl-CoAs, DAGs, and ceramides from liver by liquid chromatography-MS/MS have been described previously (21, 44, 45). DAG fractionation into the membrane and cytosolic lipid droplet compartments was done as previously reported (19). Perilipin was measured by Western blotting (Cell Signaling Technology) to confirm the lipid droplet compartment (46). Detailed methods for experiments are provided in *SI Materials and Methods*.

PKC Membrane Translocation Assay. Membrane translocation for the different PKC isoforms (PKC-α, -β, -ε, -δ, -θ, -η, -λ, –ι, -ζ, and -γ) was performed as described previously (47). Both membrane and cytosol proteins were detected on the same film with enhanced chemiluminescense at the same exposure time. PKC translocation was expressed as the ratio of arbitrary units of membrane bands over cytosol bands. Membrane band density was corrected by sodium potassium ATPase band density (Abcam), and cytosolic band density was corrected by GAPDH band density (Cell Signaling). Detailed methods for experiments are provided in *SI Materials and Methods*.

RT-PCR and Western Blotting for ER Stress Markers. ER stress markers were assessed by real-time PCR and Western blotting. For real-time PCR, total RNA was extracted from ∼15 mg liver using RNeasy mini kit (Qiagen). RNA was reverse-transcribed into cDNA with the use of M-MuLV Reverse Transcriptase (New England Biolabs). The abundance of transcripts was assessed by real-time PCR on an Applied Biosystems 7500 Fast Real-Time PCR System (Applied Biosystems) with a SYBR Green detection system (Stratagene). The expression data for each gene of interest were normalized for the efficiency of amplification with TATA box binding protein mRNA as the invariant control, which was determined by a standard curve included on each run (48). Primer sequences are provided in Table S5. For the Western blotting, proteins were extracted using ∼50 mg liver. Liver proteins were compartmentalized into three fractions, namely mitochondria plus nucleus, cytoplasm, and microsomes as previously reported (49, 50). Detailed methods for experiments are provided in *SI Materials and Methods*. BiP was detected with microsome fraction, ATF6, eIF2α, and JNK were detected with cytoplasm fraction, and CHOP was detected with mitochondria plus nucleus fraction. Microsome bands were corrected by calnexin, mitochondria plus nucleus bands were corrected by voltage-dependent anion

channels, and cytoplasm bands were corrected by β-actin or GAPDH. Cleaved ATF6 proteins were assessed between 50–70 and 36 kDa (51, 52). BiP, eIF2α, phosphorylated eIF2α (Ser51), GAPDH, JNK, phosphorylated JNK (Thr183/Tyr185), CHOP, and voltage-dependent anion channel antibodies were purchased from Cell Signaling Technology. ATF6 antibody was purchased from IMGENEX. β-actin antibody was purchased from Sigma.

Cytokine Measurements. Plasma cytokines were measured using multiplex ELISA (Meso-Scale Discovery) (53), and hepatic cytokine mRNA expression was measured by RT-PCR.

Laboratory Tests. HOMA-IR was calculated as previously described (17). High molecular weight adiponectin was measured with an ELISA kit (Millipore). hsCRP was measured with an hsCRP kit (King Diagnostics Inc.).

Lipidomics Analysis. Lipidomics analyses were done as previously described (54). Data were compared using ANOVA with the Bonferroni posthoc test.

Statistical Analysis. Linear regression analysis of the data was performed using Graph-Pad Prism 5.0. All data are expressed as mean (SD) unless otherwise indicated. *P* values less than 0.05 were considered significant.

ACKNOWLEDGMENTS. We thank Ralph Jacob Aida Groszmann, and Cathy Zou for their technical assistance and all the volunteers for their participation in these studies. This research was supported by US Public Health Service Grants R24 DK-085638, R01 DK-49230, R01 AG-23686, and UL1 RR-024139, a Manpei Suzuki Diabetes Foundation Fellowship (to N.K.), Distinguished Clinical Scientist Awards from the American Diabetes Association (to K.F.P. and G.I.S.), and a Veterans Affairs Merit Grant (to V.T.S.).

1. Grundy SM (2008) Metabolic syndrome pandemic. *Arterioscler Thromb Vasc Biol* 28: 629–636.
2. Wild S, Roglic G, Green A, Sicree R, King H (2004) Global prevalence of diabetes: Estimates for the year 2000 and projections for 2030. *Diabetes Care* 27:1047–1053.
3. Cheung O, Sanyal AJ (2010) Recent advances in nonalcoholic fatty liver disease. *Curr Opin Gastroenterol* 26:202–208.
4. Shulman GI (2000) Cellular mechanisms of insulin resistance. *J Clin Invest* 106:171–176.
5. Savage DB, Semple RK (2010) Recent insights into fatty liver, metabolic dyslipidaemia and their links to insulin resistance. *Curr Opin Lipidol* 21:329–336.
6. Samuel VT, Petersen KF, Shulman GI (2010) Lipid-induced insulin resistance: Unravelling the mechanism. *Lancet* 375:2267–2277.
7. Dowman JK, Tomlinson JW, Newsome PN (2010) Pathogenesis of non-alcoholic fatty liver disease. *QJM* 103:71–83.
8. Schmitz-Peiffer C, Biden TJ (2008) Protein kinase C function in muscle, liver, and beta-cells and its therapeutic implications for type 2 diabetes. *Diabetes* 57:1774–1783.
9. Samuel VT, et al. (2004) Mechanism of hepatic insulin resistance in non-alcoholic fatty liver disease. *J Biol Chem* 279:32345–32353.
10. Schmitz-Peiffer C (2010) Targeting ceramide synthesis to reverse insulin resistance. *Diabetes* 59:2351–2353.
11. Summers SA (2006) Ceramides in insulin resistance and lipotoxicity. *Prog Lipid Res* 45: 42–72.
12. Ussher JR, et al. (2010) Inhibition of de novo ceramide synthesis reverses diet-induced insulin resistance and enhances whole-body oxygen consumption. *Diabetes* 59: 2453–2464.
13. Tilg H, Moschen AR (2008) Inflammatory mechanisms in the regulation of insulin resistance. *Mol Med* 14:222–231.
14. Hotamisligil GS (2010) Endoplasmic reticulum stress and the inflammatory basis of metabolic disease. *Cell* 140:900–917.
15. Solinas G, Karin M (2010) JNK1 and IKKbeta: Molecular links between obesity and metabolic dysfunction. *FASEB J* 24:2596–2611.
16. Ozcan U, et al. (2004) Endoplasmic reticulum stress links obesity, insulin action, and type 2 diabetes. *Science* 306:457–461.
17. Matthews DR, et al. (1985) Homeostasis model assessment: Insulin resistance and beta-cell function from fasting plasma glucose and insulin concentrations in man. *Diabetologia* 28:412–419.
18. Bravata DM, et al. (2004) Two measures of insulin sensitivity provided similar information in a U.S. population. *J Clin Epidemiol* 57:1214–1217.
19. Bogan JS, McKee AE, Lodish HF (2001) Insulin-responsive compartments containing GLUT4 in 3T3-L1 and CHO cells: Regulation by amino acid concentrations. *Mol Cell Biol* 21:4785–4806.
20. Griffin ME, et al. (1999) Free fatty acid-induced insulin resistance is associated with activation of protein kinase C theta and alterations in the insulin signaling cascade. *Diabetes* 48:1270–1274.
21. Yu C, et al. (2002) Mechanism by which fatty acids inhibit insulin activation of insulin receptor substrate-1 (IRS-1)-associated phosphatidylinositol 3-kinase activity in muscle. *J Biol Chem* 277:50230–50236.
22. Shoelson SE, Herrero L, Naaz A (2007) Obesity, inflammation, and insulin resistance. *Gastroenterology* 132:2169–2180.
23. Olefsky JM, Glass CK (2010) Macrophages, inflammation, and insulin resistance. *Annu Rev Physiol* 72:219–246.
24. Kim JK, et al. (2001) Tissue-specific overexpression of lipoprotein lipase causes tissue-specific insulin resistance. *Proc Natl Acad Sci USA* 98:7522–7527.
25. Samuel VT, et al. (2007) Inhibition of protein kinase Cepsilon prevents hepatic insulin resistance in nonalcoholic fatty liver disease. *J Clin Invest* 117:739–745.
26. Neschen S, et al. (2005) Prevention of hepatic steatosis and hepatic insulin resistance in mitochondrial acyl-CoA:glycerol-sn-3-phosphate acyltransferase 1 knockout mice. *Cell Metab* 2:55–65.
27. Petersen KF, et al. (2006) Increased prevalence of insulin resistance and nonalcoholic fatty liver disease in Asian-Indian men. *Proc Natl Acad Sci USA* 103:18273–18277.
28. Liu L, et al. (2007) Upregulation of myocellular DGAT1 augments triglyceride synthesis in skeletal muscle and protects against fat-induced insulin resistance. *J Clin Invest* 117: 1679–1689.
29. Holland WL, Summers SA (2008) Sphingolipids, insulin resistance, and metabolic disease: New insights from in vivo manipulation of sphingolipid metabolism. *Endocr Rev* 29:381–402.
30. Fabbrini E, Sullivan S, Klein S (2010) Obesity and nonalcoholic fatty liver disease: Biochemical, metabolic, and clinical implications. *Hepatology* 51:679–689.
31. DeFronzo RA (2010) Insulin resistance, lipotoxicity, type 2 diabetes and atherosclerosis: The missing links. The Claude Bernard Lecture 2009. *Diabetologia* 53:1270–1287.
32. Skovbro M, et al. (2008) Human skeletal muscle ceramide content is not a major factor in muscle insulin sensitivity. *Diabetologia* 51:1253–1260.
33. Considine RV, et al. (1995) Protein kinase C is increased in the liver of humans and rats with non-insulin-dependent diabetes mellitus: An alteration not due to hyperglycemia. *J Clin Invest* 95:2938–2944.
34. Gregor MF, et al. (2009) Endoplasmic reticulum stress is reduced in tissues of obese subjects after weight loss. *Diabetes* 58:693–700.
35. Timpson NJ, et al. (2005) C-reactive protein and its role in metabolic syndrome: Mendelian randomisation study. *Lancet* 366:1954–1959.
36. Bajaj M, et al. (2005) Effect of a sustained reduction in plasma free fatty acid concentration on intramuscular long-chain fatty Acyl-CoAs and insulin action in type 2 diabetic patients. *Diabetes* 54:3148–3153.
37. Petersen KF, et al. (2005) Reversal of nonalcoholic hepatic steatosis, hepatic insulin resistance, and hyperglycemia by moderate weight reduction in patients with type 2 diabetes. *Diabetes* 54:603–608.
38. Petersen KF, et al. (2002) Leptin reverses insulin resistance and hepatic steatosis in patients with severe lipodystrophy. *J Clin Invest* 109:1345–1350.
39. Korenblat KM, Fabbrini E, Mohammed BS, Klein S (2008) Liver, muscle, and adipose tissue insulin action is directly related to intrahepatic triglyceride content in obese subjects. *Gastroenterology* 134:1369–1375.
40. Kotronen A, Juurinen L, Tiikkainen M, Vehkavaara S, Yki-Järvinen H (2008) Increased liver fat, impaired insulin clearance, and hepatic and adipose tissue insulin resistance in type 2 diabetes. *Gastroenterology* 135:122–130.
41. Chu X, et al. (2008) Association of morbid obesity with FTO and INSIG2 allelic variants. *Arch Surg* 143:235–240.
42. Kleiner DE, et al. (2005) Design and validation of a histological scoring system for nonalcoholic fatty liver disease. *Hepatology* 41:1313–1321.
43. Storlien LH, et al. (1991) Influence of dietary fat composition on development of insulin resistance in rats. Relationship to muscle triglyceride and omega-3 fatty acids in muscle phospholipid. *Diabetes* 40:280–289.
44. Neschen S, et al. (2002) Contrasting effects of fish oil and safflower oil on hepatic peroxisomal and tissue lipid content. *Am J Physiol Endocrinol Metab* 282:E395–E401.
45. Bligh EG, Dyer WJ (1959) A rapid method of total lipid extraction and purification. *Can J Biochem Physiol* 37:911–917.
46. Brasaemle DL (2007) Thematic review series: Adipocyte biology. The perilipin family of structural lipid droplet proteins: Stabilization of lipid droplets and control of lipolysis. *J Lipid Res* 48:2547–2559.
47. Qu X, Seale JP, Donnelly R (1999) Tissue and isoform-selective activation of protein kinase C in insulin-resistant obese Zucker rats—effects of feeding. *J Endocrinol* 162:207–214.
48. Pfaffl MW (2001) A new mathematical model for relative quantification in real-time RT-PCR. *Nucleic Acids Res* 29:e45.
49. Wiese TJ, Lambeth DO, Ray PD (1991) The intracellular distribution and activities of phosphoenolpyruvate carboxykinase isozymes in various tissues of several mammals and birds. *Comp Biochem Physiol B* 100:297–302.
50. Petrescu I, et al. (1979) Determination of phosphoenolpyruvate carboxykinase activity with deoxyguanosine 5′-diphosphate as nucleotide substrate. *Anal Biochem* 96:279–281.
51. Luo S, Lee AS (2002) Requirement of the p38 mitogen-activated protein kinase signalling pathway for the induction of the 78 kDa glucose-regulated protein/immunoglobulin heavy-chain binding protein by azetidine stress: Activating transcription factor 6 as a target for stress-induced phosphorylation. *Biochem J* 366:787–795.
52. Mao W, et al. (2007) Cardiomyocyte apoptosis in autoimmune cardiomyopathy: Mediated via endoplasmic reticulum stress and exaggerated by norepinephrine. *Am J Physiol Heart Circ Physiol* 293:H1636–H1645.
53. Ford ES, et al. (2010) Traditional risk factors and D-dimer predict incident cardiovascular disease events in chronic HIV infection. *AIDS* 24:1509–1517.
54. Yang K, Cheng H, Gross RW, Han X (2009) Automated lipid identification and quantification by multidimensional mass spectrometry-based shotgun lipidomics. *Anal Chem* 81:4356–4368.